



Diatom-inferred centennial-millennial postglacial climate change in the Pacific Northwest of North America

Joanne Egan · William J. Fletcher ·
Timothy E. H. Allott

Received: 21 September 2021 / Accepted: 29 April 2022
© The Author(s) 2022

Abstract A diatom record from Moss Lake, Washington, USA spans the last 14,500 cal year and revealed Holocene climate change in the Pacific Northwest (PNW), including evidence for periodicities related to ocean-atmosphere teleconnections and/or variations in solar output. Three main climate phases were identified: (i) Late Pleistocene to early Greenlandian (until 10,800 cal year BP, spanning GI-1, GS-1), with a cold climate and low diatom abundance; (ii) early Greenlandian to Northgrippian (10,800–7500 cal year BP), shifting to a warmer climate; and (iii) late Northgrippian and Meghalayan from 7500 cal year BP onwards, with a cooler, moist climate. These climate shifts are in good agreement with the pollen record from the same core and other regional studies. Fluctuations in *Discostella pseudotelligera* and *Aulacoseira* taxa suggest climate cycles of different frequency and amplitude throughout the

record. Spectral and wavelet analyses revealed periodicities of approximately 1400 and 400–500 years. We interpret the ~1400-year and ~400–500-year cycles to reflect alternating periods of enhanced (and reduced) convective mixing in the water column, associated with increased (and decreased) storms, resulting from ocean–atmosphere teleconnections in the wider Pacific region. The ~1400-year periodicity is evident throughout the Late Pleistocene and late Northgrippian/Meghalayan, reflecting high-amplitude millennial shifts from periods of stable thermal stratification of the water column (weak wind intensity) to periods of convective mixing (high wind intensity). The millennial cycle diminishes during the Greenlandian, in association with the boreal summer insolation maximum, consistent with suppression of ENSO-like dynamics by enhanced trade winds. Ocean–atmosphere teleconnection suppression is recorded throughout the PNW, but there is a time discrepancy with other records, some that reveal suppression during the Greenlandian and others during the Northgrippian, suggesting endogenic processes may also modulate the Moss Lake diatom record. The large amplitude of millennial variability indicated by the lake data suggests that regional climate in the PNW was characterised over the longer term by shifting influences of ocean–atmosphere dynamics and that an improved understanding of the external forcing is necessary for understanding past and future climate conditions in western North America.

Supplementary Information The online version contains supplementary material available at <https://doi.org/10.1007/s10933-022-00244-x>.

J. Egan (✉)
Department of Geography and Geology, Edge Hill
University, St Helens Road, Ormskirk L39 4QP,
Lancashire, UK
e-mail: eganj@edgehill.ac.uk

W. J. Fletcher · T. E. H. Allott
Department of Geography, School of Environment,
Education and Development, University of Manchester,
Oxford Road, Manchester M13 9PL, UK

Keywords Diatoms · Pacific Northwest · Paleoclimate · Spectral analysis · Teleconnections · Wavelet analysis

Introduction

Ocean–atmosphere interactions have a major influence on global climate. In the Pacific Northwest (PNW) of North America, the climate is influenced by multiple ocean–atmosphere teleconnections that vary seasonally, annually and decadal. Important teleconnections that prevail in the Pacific region are the Pacific Decadal Oscillation (PDO), El Niño–Southern Oscillation (ENSO) and the Northern Annular Mode (NAM), which can have severe and wide-reaching influences on ecosystems (Mantua et al. 1997; Iizumi et al. 2014). Furthermore, across the PNW, the North Pacific High (NPH) and the Aleutian Low (AL) modulate the strong seasonality

in the region. The position and strength of the AL exert the strongest climatic influence on the PNW and generate storm systems that are carried across North America (Stone et al. 2016). There is a strong relationship between the AL and the phase of the aforementioned teleconnections (Rodionov et al. 2007). For example, wet periods often occur during La Niña events and negative PDO phases when the AL weakens and shifts westward, which causes the meridional flow to weaken and the zonal flow to intensify, routing storm tracks into the continental interior (Rodionov et al. 2005) and impacting the PNW (Fig. 1, bottom right). In contrast, during El Niño events and positive PDO phases, the AL intensifies and shifts eastward and enhances the meridional flow, leading to a more northern storm track that impacts Alaska and generates warmer winter temperatures in the PNW (Rodionov et al. 2005; Stone et al. 2016) (Fig. 1, bottom right). On longer timescales, the position and intensity of the AL has shifted, and this has been

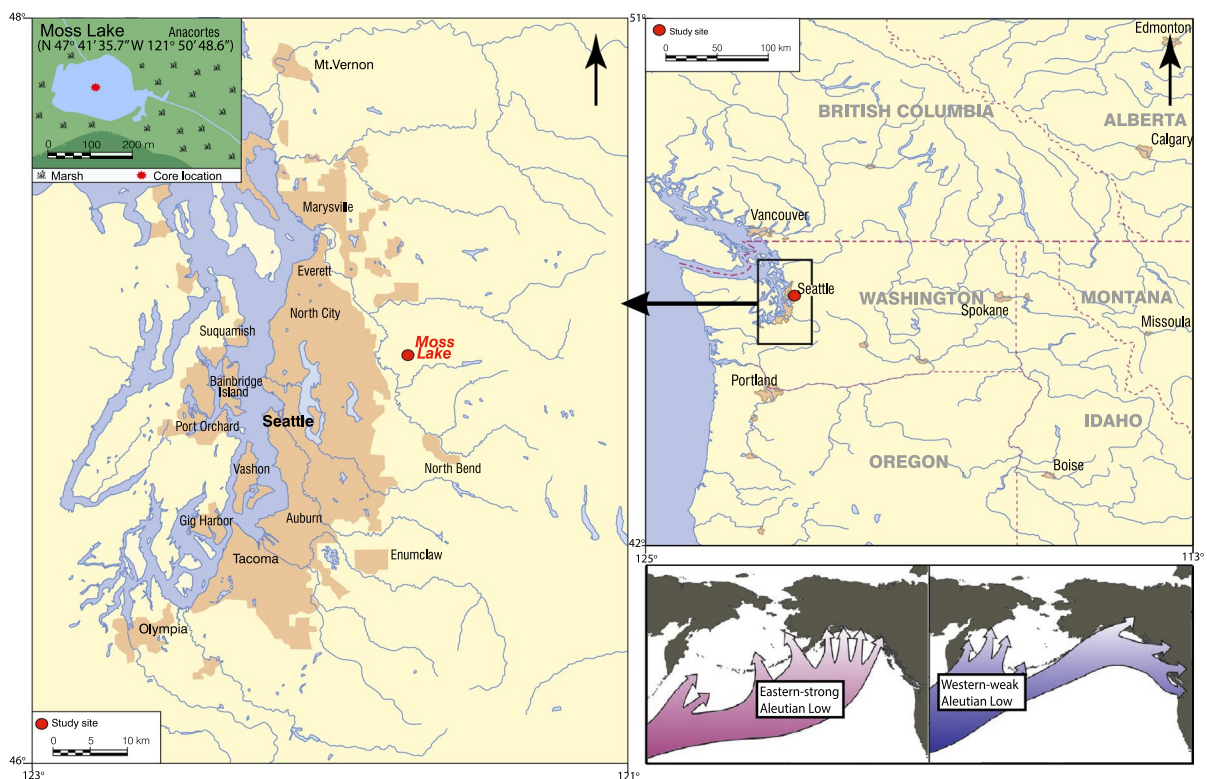


Fig. 1 Left: Location of Moss Lake and an inset map of Moss Lake (top left) indicates the coring location. Right: location of Moss Lake in relation to the PNW, and bottom right: Position and influence of the Aleutian Low on storm tracks (adapted

from Stone et al. 2016); Eastern/strong Aleutian Low sends storms north to Alaska (left) and Western/weak Aleutian Low sends storms to the continental interior; to southern Canada and the PNW (right)

associated with variations in sea surface temperatures in the North Pacific (Stone et al. 2016) that can influence PNW climate and continental ecosystems (Barron and Anderson 2011).

Our understanding of ocean–atmosphere teleconnections stems primarily from historical observations. However, investigations of paleoclimate change in climatically sensitive regions can expand our knowledge and understanding of internal (ocean–atmosphere teleconnections) and external (solar variability) climate drivers across longer timescales. In the PNW, reconstructions of climate and environmental change have commonly been attained from terrestrial records, especially pollen records (Whitlock 1992; Prichard et al. 2009; Courtney Mustaphi and Pisaric 2014). The palynological records highlight the complexity of inferring past climate change because palynological signals are influenced by other factors such as fire, soil development and local vegetation dynamics. Nevertheless, the prevailing regional vegetation and climate shifts in the Holocene were determined from these studies (Electronic Supplementary Material [ESM] Fig. S1). The climate was cold and dry until 12,000 cal year BP, with a shift from *Pinus*-dominated forests to *Pseudotsuga*. Warming occurred throughout the Greenlandian, reaching maximum warmth ~8000 cal year BP. During that time, the forest assemblage became more diverse, with the establishment and increases in *Tsuga* and Cupressaceae. These taxa increased rapidly from 5000 cal year BP, as the climate cooled and became moister. The observed changes occurred on sub-orbital (multi-millennial) scales, with little evidence to constrain fluctuating or cyclical changes associated with ocean–atmosphere teleconnections and solar variability.

Lakes are sensitive to climate and environmental changes, and lacustrine sediments have been used to reconstruct past Holocene climates (Galloway et al. 2013). Diatoms are especially valuable for inferring past climate conditions, as diatom communities respond to variations in pH, salinity, nutrient status, lake level (Saros et al. 2012), the duration and timing of ice cover (Lotter and Bigler 2000), water column stability, and thermal stratification (Saros et al. 2012; Stone et al. 2016, 2019). Since these factors may be influenced by temperature and precipitation (Rühland et al. 2003), diatoms also provide indirect evidence of past climate changes. Diatom records have an

advantage over some other bioindicators because of their short lifespans and rapid generational turnover, which makes them ideal for recording abrupt climate changes. Studies in alpine lakes in southern British Columbia, Canada, reported diatom-inferred climate shifts that were not observed in pollen records (Bennett et al. 2001; Karst-Riddoch et al. 2005). Diatoms have the potential to record the influence of ocean–atmosphere teleconnections on climate, as storms may cause convective mixing of the epilimnion, which affects the thermal structure of the lake and thus influences important lake properties such as nutrient status and light availability (Stone et al. 2016).

Previous paleoclimate studies in the region elucidated that ocean–atmosphere interactions occur on the full range of timescales, from seasonal to millennial (Moy et al. 2002; Ersek et al. 2012; Jiménez-Moreno et al. 2019). Many of those studies suggested associations with the PDO (Barron and Anderson 2011), ENSO (Moy et al. 2002; Anderson et al. 2005; Kennett et al. 2007; Steinman et al. 2014, 2016; Jiménez-Moreno et al. 2019) and the AL (Stone et al. 2016). Several studies also proposed solar activity variation as a driver for change in the Pacific climate system (Moy et al. 2002; Marchitto et al. 2010; Ersek et al. 2012; Gavin et al. 2011; Galloway et al. 2013). Indeed, the Northwest Pacific region might be an important global amplifier for solar variability (Emile-Geay et al. 2007). Specific to the PNW, Ersek et al. (2012) and Steinman et al. (2014, 2016) indicated millennial-scale climate change and suggested that the changes arise from mechanisms similar to ENSO and/or PDO. Extreme transitions in the climatic and hydrological phases also appear to correlate with variations in solar activity, with extreme cold and wet events correlated to high solar forcing (low global ^{10}Be flux and ^{14}C production) and vice versa, which then influences winter storm tracks (Ersek et al. 2012; Steinman et al. 2014). However, the wider environmental impact of these transitions is poorly understood. Therefore, this study investigated the extreme events that appear to reoccur on millennial timescales and persist for 100s of years (Ersek et al. 2012).

There remains a need for highly resolved (multi-centennial-scale or better) and robustly dated paleoenvironmental sequences from the PNW to test for past evidence of ocean–atmosphere teleconnections and

their variations throughout the Holocene. Here we present a new Holocene diatom record from Moss Lake (N 47° 41' 35.7" W 121° 50' 48.6"), in the foothills of the Cascade Mountains in the state of Washington, USA (Fig. 1). We compare our findings with the pollen-based record of vegetation history in the surrounding conifer forest, obtained from the same core (Egan et al. 2016). This area is sensitive to the influences of the ENSO, PDO, AL and NPH. The area experiences wind anomalies associated with winter storm tracks that are modulated by the position of the AL (Stone et al. 2016). Moss Lake has a diameter of approximately 200 m, a maximum depth of 4.5 m and a catchment area of 0.62 km². The lake is a freshwater, slightly acidic, oligotrophic lake, typical of the region. The site is located at an elevation of 158 m.a.s.l., in a mixed conifer forest within the Tolt River Basin (Fig. 1). Moss Lake appears to have developed in a former glacial depression (Rigg 1958), evidenced by basal glaciomarine deposits (Fig. 2).

Thus, this lake is suitable for reconstructing environmental change from the time of regional deglaciation to present.

The aims of this study were to determine whether Moss Lake was sensitive to and recorded extreme millennial- and multi-centennial-scale macro-climate signals, and to elucidate the potential internal and/or external controls on the diatom assemblage and lake system. It was not the goal of this paper to determine the specific mechanisms that drive the climate signals (such as ENSO, PDO, AL), but rather, to explore the possibility that the lacustrine diatom assemblage recorded ocean–atmosphere teleconnections and millennial/multi-centennial-scale climate variability. To our knowledge, this study yielded one of the first records of Late Glacial and Holocene climate-related environmental change in the region derived from lake sediment variables, and one of the few sites in the PNW that offers insights into rapid Holocene climate changes.

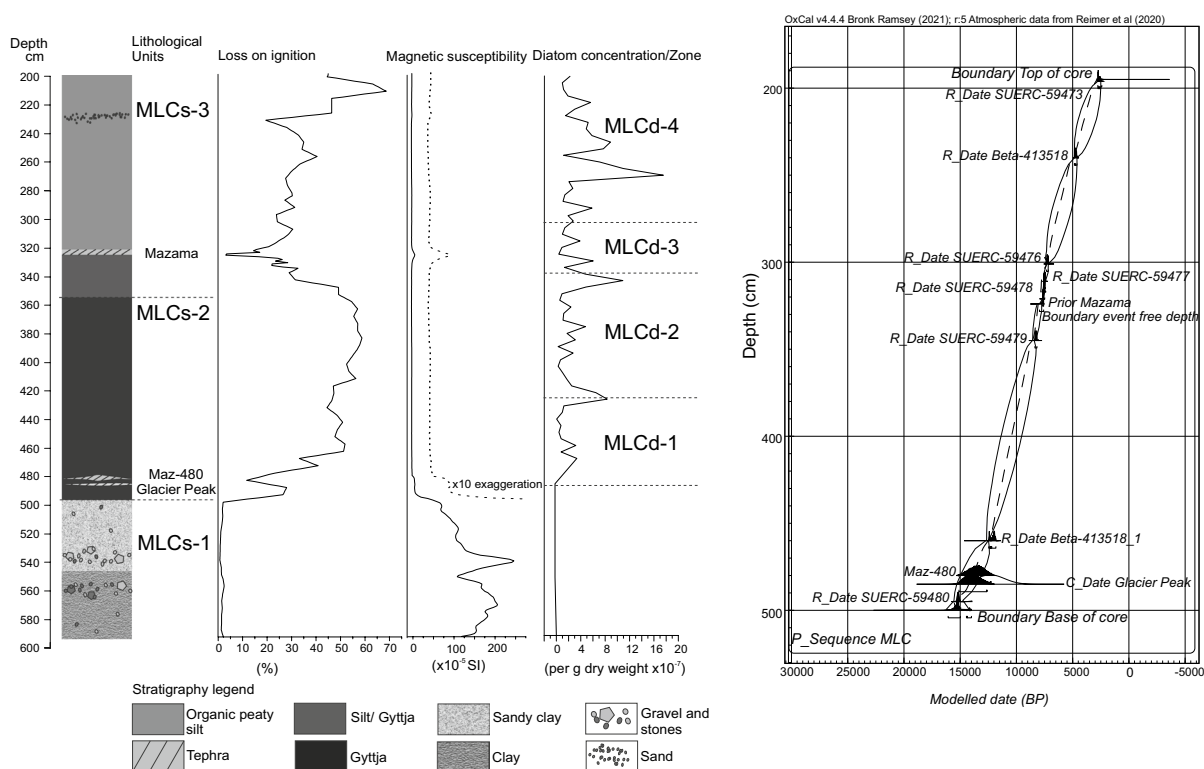


Fig. 2 Stratigraphy of MLC including sediment description, LOI, magnetic susceptibility, and diatom concentration and diatom zones (left); Bayesian age-depth [OxCal v.4.4 (Bronk Ramsey 2021)] model for MLC derived from the comparison

of the radiocarbon ages calibrated using the IntCal20 (Reimer et al. 2020) dataset. 95% confidence interval/boundary of the deposition model. Dashed line displays the median (right)

Materials and methods

A 4-m core was collected in May 2014 from the deepest part of Moss Lake (4.5 m established with an echo sounder) with a modified Livingstone corer. Core retrieval began at 200 cm because of the exceptionally loose, unconsolidated nature of the material above, and coring stopped at 6 m sediment depth, when we encountered gravelly clays. The core was extruded into plastic guttering, wrapped in cling film for transport, and stored in the cold room (dark, 4 °C) at The University of Manchester, UK.

Stratigraphic analyses and chronology

Stratigraphic and chronological data presented here were originally provided in Egan et al. (2016), where details of the methods can be found. Magnetic susceptibility was measured at room temperature and low frequency (0.47 kHz) using the MS2C scanner of a Bartington Instruments Ltd MS2 meter, to determine allochthonous inputs. Measurements were taken for 10 s for each 1-cm section. Organic matter and carbonate content (an indicator of potential hard-water effect on radiocarbon dating) were estimated by loss-on-ignition (LOI), i.e., heating of dry sediment at 550 °C for organic matter content and 925 °C for carbonate content (Dean 1974). Samples were taken every 1 cm throughout the sequence.

Accelerator mass spectrometry (AMS) radiocarbon dates were obtained for eight bulk sediment samples (pre-treated with HCl) from Moss Lake (Egan et al. 2016). There was a lack of identifiable macrofossils or macro-charcoal fragments suitable for dating, thus bulk sediments were used. We infer from the negligible carbonate content that significant hard-water dating errors are unlikely. Radiocarbon dates were calibrated to calendar years (cal year BP) using OxCal v.4.4 (Bronk Ramsey 2021), and the IntCal20 calibration curve (Reimer et al. 2020). Bayesian modelling was used to create an age-depth model using a *P_sequence* deposition model in OxCal v.4.4. The model included an “event-free depth scale” (Staff et al. 2011) for the instantaneous deposition of a 4-cm-thick tephra layer and interpolated ages every 1 cm (Egan et al. 2016). There are three visible tephra deposits in the core. The tephrae were geochemically identified on the JEOL-JXA8600 electron microprobe at the Research Laboratory for Archaeology

and the History of Art, University of Oxford (Egan et al. 2016). They are geochemically attributed to Glacier Peak (485 cm, <1 cm thick), Maz-480 (480 cm, <1 cm thick) (a potentially Late Pleistocene eruption of Mount Mazama), and the climactic Holocene eruption of Mount Mazama (324 cm, 4 cm thick). The age of the Mount Mazama tephra is well constrained to 7682–7584 cal year BP (Egan et al. 2015), strengthening the age-depth model and adding confidence in the radiocarbon-based chronology.

Diatom analysis

Contiguous samples were taken every 5 cm, representing one sample for every ~100–200 years of sediment accumulation, ideal for determining the nature, timing and duration of multi-centennial and millennial-scale climate changes. Diatom preparation followed standard procedures, described in Egan et al. (2019). Diatom concentration was determined by adding microspheres (2 ml of 5.01×10^6 per 0.01 g dry weight of sediment). Samples were diluted and mounted using Naphrax®. Diatoms were identified and counted at $\times 1000$ magnification. Identification was aided by the website “Diatoms.org” (Spaulding et al. 2021) and identification keys (Krammer and Lange-Bertalot 1991, 1999a, b). A minimum of 300 diatom frustules was counted per sample. Psimpoll v.4.27 was used for the diatom diagram and the number of zones and their placement were determined using the broken stick model and optimal splitting by information content (Bennett 2007).

Diatom-based proxy for wind-driven convective mixing

An index representative of convective mixing within the lake, and representing storm influence on the area, was created using the ratio of planktonic *Discostella pseudostelligera* (Hust.) Houk and Klee 2004 and tychoplanktonic *Aulacoseira* taxa, *D. pseudostelligera*: *Aulacoseira* (D:A). The ratio was calculated using the following equation: $D:A = \frac{Aulacoseira}{Aulacoseira + D. pseudostelligera}$. It is recognised that storms can generate mixing within the epilimnion, which affects the depths of the thermocline and thus thermal stratification of the lake (Wang et al. 2012; Stone et al. 2016, 2019). Changes in the thermal stratification of a lake influence physical and

physico-chemical properties of the water, which can influence the structure and composition of the plankton. Studies by Saros et al. (2012) and Stone et al. (2016, 2019) reported on the influence of mixing depths on different diatom species and recognised that *Discostella* and *Aulacoseira* species are particularly effective indicators of convective mixing. The ecological characteristics of the D:A ratio suggest changes in convective mixing within the lake in response to the intensity and frequency of storms. A higher occurrence of *Aulacoseira* taxa should occur if there is increased wave action and convective mixing, enabling surface water to mix with nutrient-rich water from below and enabling the diatoms to remain suspended in the water column (Wang et al. 2012), whilst higher abundances of *D. pseudostelligera* reflect a stable water column that is thermally stratified and has shallow mixing depths of ~4 m (Saros et al. 2012). *D. pseudostelligera* should predominate under stable climate conditions with weak winds (Stone et al. 2016), whereas *Aulacoseira* taxa should predominate in well-mixed water under windier conditions. In this record, fluctuations in the relative abundance of *D. pseudostelligera* and *Aulacoseira* taxa reflect changes in the intensity of wind-driven mixing that influence thermal stratification of the water column, which in turn may be generated from westerly storm tracks associated with the position of the AL (Fig. 1) and other ocean–atmosphere teleconnections. The shallow lake bathymetry and open-lake setting make the site ideal to record mixing, as increases in wind intensity can easily disturb the water column. It is important to note that *Aulacoseira* taxa and *D. pseudostelligera* have temperature preferences, too, with *D. pseudostelligera* preferring warmer (Descamps-Julien and Gonzalez 2005) temperatures. *Aulacoseira* taxa have wider temperature preferences and are highly influenced by nutrient concentrations (Bennion et al. 2012). It is possible that these diatoms responded to temperature changes associated with the ocean–atmosphere teleconnections, as the storm tracks, directed toward the north during El Niño, positive PDO and intense AL, generate warmer winter temperatures for the PNW, thus causing an increase in *D. pseudostelligera*. However, given uncertainties about the *Aulacoseira* taxa, and the small size of Moss Lake, it is more likely that these diatoms were influenced by wind-driven mixing, which also correlates well with nutrient concentrations.

Time series analysis determined if significant periodicities were recorded in the lake mixing index of Moss Lake. For the purposes of removing orbital-to-sub-orbital-scale trends prior to spectral analyses, the D:A ratio was detrended by fitting a 3rd-order polynomial model in PAST v4.03 (Hammer et al. 2001). The order of the model was chosen to ensure removal of “cycles” that are longer than half of the period covered.

RedFit spectral analysis of the detrended D:A series was used, as this method is suitable for irregularly spaced and noisy data (Schulz and Mudelsee 2002). RedFit undertakes a spectral analysis using the Lomb-Scargle Fourier transform, and the resulting spectrum is bias-corrected using spectra computed from simulated first-order autoregressive (AR1) series and the theoretical AR1 spectrum. The AR1 process provides a good null hypothesis for a “red-noise” origin of variability in a paleoclimate time series. RedFit estimates the AR1 parameter from unevenly spaced times series data, without interpolation, and by comparison with the spectrum of the time series, permits identification of significant cyclicities that are inconsistent with the AR1 process (Schulz and Mudelsee 2002). For the RedFit calculations, a Welch’s Overlapping Segment Averaging (WOSA) approach was used, with selection of the “Welch” window, which provides a good compromise between smoothing and peak detection, three overlapping segments, and an oversampling factor (ofac) of ten. The maximum frequency (hifac) was set to the Nyquist frequency, which is the highest frequency information that can be obtained from real data and is defined as $1/(2 \times \text{sample interval})$ (Weedon 2003), in this case $f=0.0025$, yielding a lower limit for detectable periodicities of ~400 years. A Monte Carlo simulation (1000 runs) was executed to determine the significant peaks with respect to red noise. The critical “false alarm” level of $1-(1/n)$ was calculated, where n is number of observations in each overlapping segment, which is recommended for exploratory analyses to reduce the possibility of false positives (Thomson 1990). RedFit analysis was implemented in the R package dplR v1.7.2 (Bunn et al. 2021).

Wavelet analysis is a complementary approach to spectral analysis using RedFit because the local time-scale decomposition enables the tracking of spectral characteristics as a function of time, and hence permits the detection of non-stationarity in the time

series (Torrence and Compo 1998). The detrended D:A data were interpolated to an even spacing of 200 years (close to the average sample spacing of 194 year) and zero padded to reduce edge effects. The Morlet wavelet was applied and the wavelet spectrum produced details of all the found frequencies, and their amplitude at each data point confined within a specific time interval (Weedon 2003). Significance testing was based on Monte Carlo simulations against a red-noise AR(1) null hypothesis. Significant periodicities at the 90%, 95% and 99% are reported visually on the wavelet diagram and the “cone of influence” illustrates areas where the detection of significant periodicities may be diminished because of proximity to the ends of the time series. Wavelet analysis was performed using the R package Wavelet-Comp v1.1 (Roesch and Schmidbauer 2018).

Periodic behaviour was further modelled using sinusoidal regression using the “search” function in PAST v4.03 (Hammer et al. 2001) to determine the optimum frequency, amplitude, phase and significance of one or multiple sinusoids. Graphical visualisation of low-frequency changes in the detrended D:A ratio and other paleoclimate proxies was achieved by applying a second-order Butterworth lowpass filter with frequency cut-off 1/500 year, implemented in the R package signal v0.7-7 (signal developers 2013). Datasets were padded to 500 year beyond the ends of the time series with the long-term mean value to avoid edge effects.

Results

Stratigraphy

Three major stratigraphic units (Fig. 2; MLCs1-3) were identified (Egan et al. 2016). MLCs-1 (590–495 cm) has low LOI and high magnetic susceptibility values, and consists of clays and gravels. Faceted stones are present within the two gravel units, indicative of glacial origin. MLCs-2 (495–355 cm) consists of gyttja, has greater LOI values (60%); magnetic susceptibility decreases and remains low. MLCs-3 (355–200 cm) shifts to silty gyttja. At 230 cm there is a sand layer that coincides with lower LOI and increased magnetic susceptibility. Carbonate content is <0.04% throughout. Within the tephra deposits, LOI declines to 5% and magnetic

susceptibility increases, most notably around the Mazama tephra layer at 324 cm.

Radiocarbon dates

Sediment zones MLCs-2 and MLCs-3 yielded dates extending from the Late Pleistocene (16,070–14,000 cal year BP) to the Meghalayan (3528–2515 cal year BP) (Fig. 2, ESM Table S1) (Egan et al. 2016). The most recent sediments were not collected and are thus missing from the age model. The chronology within the Holocene is well constrained, most notably at the time of tephra deposition from Mazama, with an error of ± 200 years.

Diatoms

One hundred diatom taxa were identified. Of those, 17 common taxa had relative abundances >5% in at least three sediment samples, and data from those taxa are reported here. Four significant zones were identified through statistical zonation (Fig. 3, ESM Table S2). Diatom concentration was 0 g^{-1} dry weight from 600 to 490 cm. Diatoms first appeared at 490 cm, associated with the transition to zone MLCs-2 (Fig. 2). The first diatom zone, MLCd-1, has diatom concentrations between 1×10^7 and 10×10^7 frustules g^{-1} dry weight, and is dominated by *D. pseudostelligera*, with a peak abundance of 70%. In MLCd-2, there is a slight increase in diatom concentration to between 1×10^7 and 12×10^7 frustules g^{-1} dry weight, and the dominance shifts from planktonic to tychoplanktonic diatoms, primarily *Pseudostaurosira brevistriata* (Grunow) Williams and Round 1988 and *Staurosira venter* (Ehrenberg) Cleve and Möller 1879, which represent up to 70% of the assemblage. In MLCd-3, the concentration decreases to between 1×10^7 and 4×10^7 frustules g^{-1} dry weight and is dominated by *D. pseudostelligera*, with peak abundance of 70%. Tychoplanktonic species decrease in MLCd-3, and *D. pseudostelligera* increases. After the Mazama tephra layer, tychoplanktonic taxa increase, and *D. pseudostelligera* decreases. MLCd-4 has the highest diatom concentrations (between 1×10^7 and 18×10^7 frustules g^{-1} dry weight), and is more variable in terms of species composition, with shifting dominance between tychoplanktonic taxa and planktonic *D. pseudostelligera*.

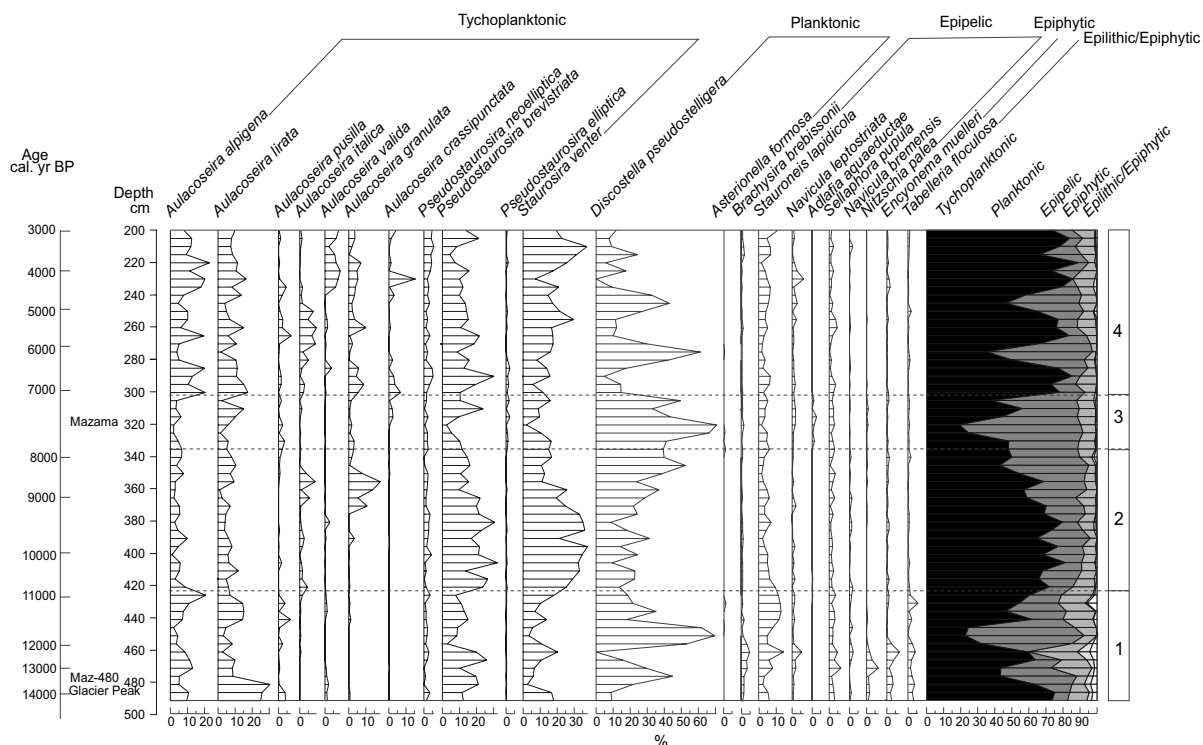


Fig. 3 Holocene diatom record from Moss Lake and diatom summary based on percentages. Diatom zones (MLCd-#) are numbered 1–4. Ages based on the age-depth model

Throughout the assemblage, there are notable shifts of *D. pseudostelligera*, tytoplanktonic *Aulacoseira* taxa, *P. brevistriata* and *S. venter* (Fig. 3), indicating a suitable data set for time series analysis. However, as described in the methods, we focused on the D:A ratio for time series analysis. Although *P. brevistriata* and *S. venter* prefer cooler temperatures (Rühland et al. 2003), they have broad climate and environmental tolerances, so the environmental interpretation of changes in their abundance is less certain.

Down-core changes in the D:A ratio reveal fluctuations throughout the Late Glacial and Holocene (Fig. 4). Both the ratio and the polynomial model illustrate three stratigraphic intervals among which there are distinct differences in the assemblages (Fig. 4c). Between 14,200 and 10,800 cal year BP, high D:A ratios predominate, with superimposed high-amplitude, millennial-scale fluctuations. Between 10,800 and 7500 cal year BP (Greenlandian and early Northgrippian), intermediate D:A ratios with low-amplitude, high-frequency fluctuations are apparent. Finally, after 7500 cal year BP

(Northgrippian and Meghalayan), millennial-scale fluctuations of high amplitude become more pronounced, with a high D:A ratio.

Spectral analyses

RedFit analysis (Fig. 5) shows a highly significant periodicity of 1386 years, which exceeds the critical false alarm significance level of 96.7%. The wavelet analysis (Fig. 6a) reveals that periodic behaviour was most pronounced in the Late Pleistocene and earliest Greenlandian (MLCd-1) and again in the Northgrippian to Meghalayan (MLCd-3 and 4), weakening in much of the intervening Greenlandian. This near-1400-year oscillation dominates the wavelet results, as seen in the average wavelet power (Fig. 6b). The best-fit sinusoidal model (Fig. 6c) has a period of 1375 years ($R^2=0.33$, $p=6.5 \times 10^{-7}$), high amplitude (0.17). Comparison of the sinusoidal model and the lowpass-filtered time series (Fig. 6c) highlights a constant phasing of the millennial fluctuation between the Late Pleistocene (MLCd-1) and

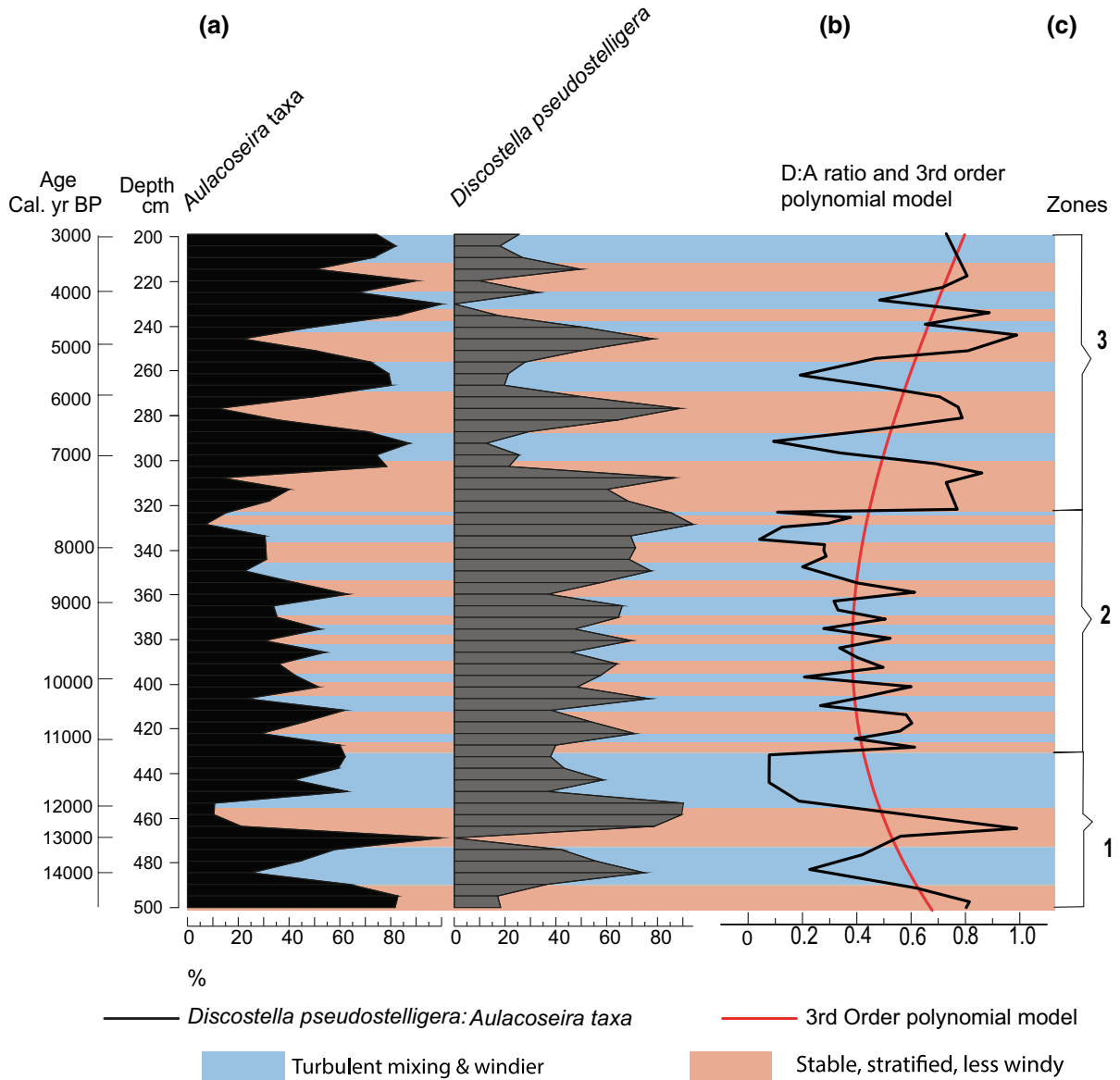


Fig. 4 Illustration of oscillations (subjective) recorded at Moss Lake **a** diatom assemblage of *Aulacoseira taxa* and *Discostella pseudostelligera*; **b** D:A ratio and polynomial model

3rd order; **c** subjective cycle zones illustrating different intensities and durations of cycles. The shading indicates the inferred changes in turbulent mixing of the water column

late Northgrippian and Meghalayan (MLCd-3 and 4). A second best-fit sinusoidal model was derived for the intervening time period, which has a period of 450 years ($R^2=0.32$, $p=0.03$) and lower amplitude (0.12). The 400–500-year fluctuations are most pronounced in the Greenlandian and early Northgrippian (11,500–8500 cal year BP), MLCd-2. This multi-centennial variability is partly reflected in the

wavelet diagram (Fig. 6a), with weak periodicity (>90% confidence) near 11,000 cal year BP. However, this variability is close to the Nyquist frequency, meaning that it may be difficult to distinguish from sample noise; this variability is also affected by regular interpolation prior to the wavelet analysis, resulting in a weaker signal than detected by the sinusoidal regression.

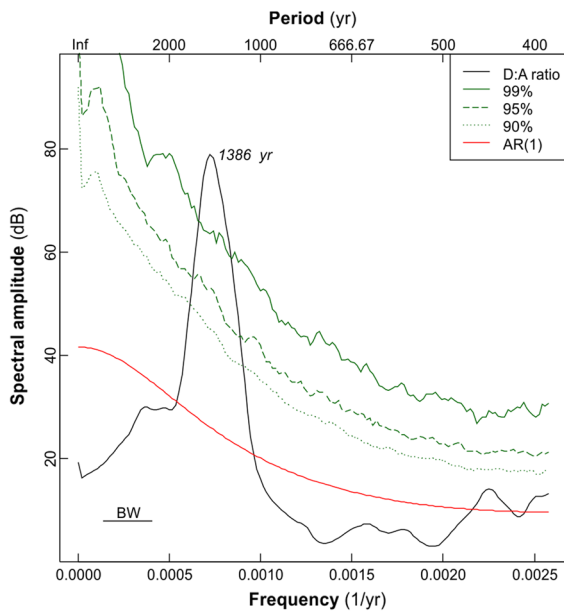


Fig. 5 RedFit spectral analysis results (Welch window and three overlapping segments), showing the bias-corrected spectrum of the detrended D:A time series (black line), theoretical red-noise AR(1) spectrum (red line) and Monte Carlo confidence limits (green lines). The spectral peak at period 1386 year is inconsistent with a red-noise origin at the 99% confidence limit, exceeding the critical false-alarm level (96.7%), which takes into account the number of observations in each. (Color figure online)

Discussion

Long-term environmental changes at Moss Lake

The sedimentological and diatom records from Moss Lake reveal major climate changes during the last 14,200 years, spanning much of the Late Glacial interstadial (GI-1), the Younger Dryas (GS-1) (BA-YD) and the Holocene (Figs. 2 and 3). Diatom zone MLCd-1 (14,200–10,800 cal year BP) (Fig. 3) represents the onset of deglaciation, with a shift from glacial clays to organic sediments and the introduction of diatoms during the Bølling–Allerød interstadial. Diatoms were absent before that time either because it was not an aquatic environment then, consistent with an origin of Moss Lake as a glacial depression that filled with water following deglaciation (Rigg 1958), or because cold conditions prevailed, with a long period of ice cover and shorter growing season that would have prevented diatom growth (Karst-Riddoch et al. 2005). Epipellic species are in relatively

high abundance in MLCd-1 (Fig. 3), as they colonised clastic inputs following deglaciation, evidenced by the higher magnetic susceptibility in MLCs-1 (Fig. 2). The two tephra deposits identified [MLC-T480 and MLC-T485, Egan et al. (2016)] may have contributed to the epipellic abundance, as these life-forms can colonise tephra deposits (Egan et al. 2019). Evidence of the Late Glacial climate oscillation (BA-YD) was identified in pollen records from Moss Lake (Egan et al. 2016), with a shift from a *Pinus*-dominated woodland (90%) starting at 14,200 cal year BP during the Bølling–Allerød interstadial (Two Creeks Interval in the USA), to a forest dominated by *Pseudotsuga menziesii* (70%) by 11,800 cal year BP, the Younger Dryas stadial (Fig. 7). This shift in vegetation occurred throughout the PNW (Whitlock 1992; Prichard et al. 2009; Courtney Mustaphi and Pisaric 2014).

MLCd-2 covers the period 10,800–7800 cal year BP, the Greenlandian and early Northgrippian. It was a period of warming and catchment stability, evidenced by the pollen record with *P. menziesii* dominating and an increase in LOI (70% organic matter). *D. pseudostelligera* dominates and is most stable in this zone, showing an increasing trend from 20 to 50%, supporting the inference for warmer climate and indicating thermal stratification of the water column (Rühland et al. 2003), a consequence of catchment stability. This was a known period of warming in North America (Whitlock 1992; Prichard et al. 2009; Courtney Mustaphi and Pisaric 2014; Egan et al. 2016). *P. brevistriata* and *S. venter* also dominate, but because of their complex taxonomy and ecological response (Schmidt et al. 2004), it is not possible to ascertain a climate signal from these species, and because of the thermal stratification of the water column, it is likely these species acted as benthic taxa, uninfluenced by climate.

From 7800 to 7000 cal year BP (MLCd-3), during the early Northgrippian, the diatom assemblage became more diverse, with the emergence or re-emergence of epipellic species *Adlafia aqueductae* (Krasske) Lange-Bertalot 1998, *Brachysira brebissonii* Ross 1986, and *Nitzschia palea* (Kützing) Smith 1856. Warmer environments create more amenable conditions for diatom growth (reduced alkalinity, increased nutrient availability, increased DOC, longer growing seasons and an increase in habitat availability) (Karst-Riddoch et al. 2005). The increase

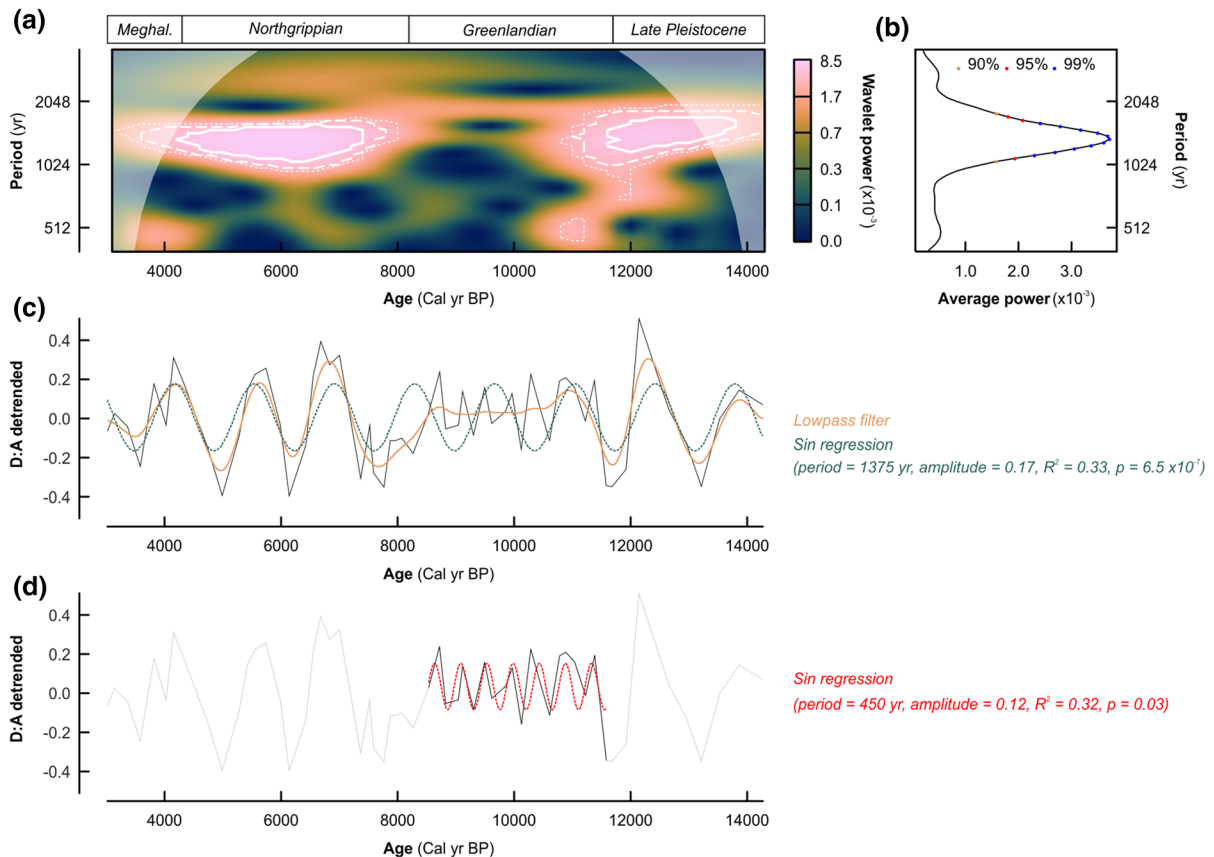


Fig. 6 Result of wavelet analysis, bandpass filter and sinusoidal regressions, showing: **a** wavelet diagram for detrended and 200-year interpolated D:A time series, annotated with the cone of influence and 90%, 95% and 99% confidence limits (dotted, dashed and solid white lines, respectively); **b** average

wavelet power; **c** 500-year lowpass filter (gold line) and best-fit sinusoid (green line, period = 1375 year) for the detrended (not interpolated) D:A data; **d** best-fit sinusoid (red line, period = 450 year) for the partial time window 11,600 cal year BP to 8500 cal year BP. (Color figure online)

in diversity of a diatom flora is recognised to follow increasing vegetation abundance and the development of forests (Bradbury et al. 2004), specifically the development of a more closed conifer forest at Moss Lake, indicated by the further increase of *Tsuga heterophylla* and emergence of Cupressaceae (Fig. 7, MLCp-3). The gradual decline in LOI suggests there was a decrease in organic input to the lake, likely related to more stable soils within the closed-forest system. This catchment stability, and thus stronger thermal stratification, is reflected in the peak of *D. pseudostelligera*, which could indicate shallow mixing depths that enabled the growth of this species (Saros et al. 2012).

MLCd-4 (7000–3000 cal year BP) corresponds to a known period of climate cooling and increasing

moisture in the region (Whitlock 1992; Courtney Mustaphi and Pisaric 2014) and reflects possible terrestrialisation of the lake and forest development within the catchment. Terrestrialisation is evidenced by the increase in organic matter in MLCs-3 (Fig. 2) and the corresponding growth of *Tsuga heterophylla*, Cupressaceae and *Equisetum* in MLCp-3, which were low in abundance before this time (Fig. 7). Increases of tycho planktonic *S. venter* and *P. brevistriata* further support terrestrialisation, as they are indicative of marsh environments (Bradbury et al. 2004). Overall, the pollen and diatom reconstructions indicate both catchment- and climate-related changes, but with the diatom record revealing more variability of a cyclical nature.

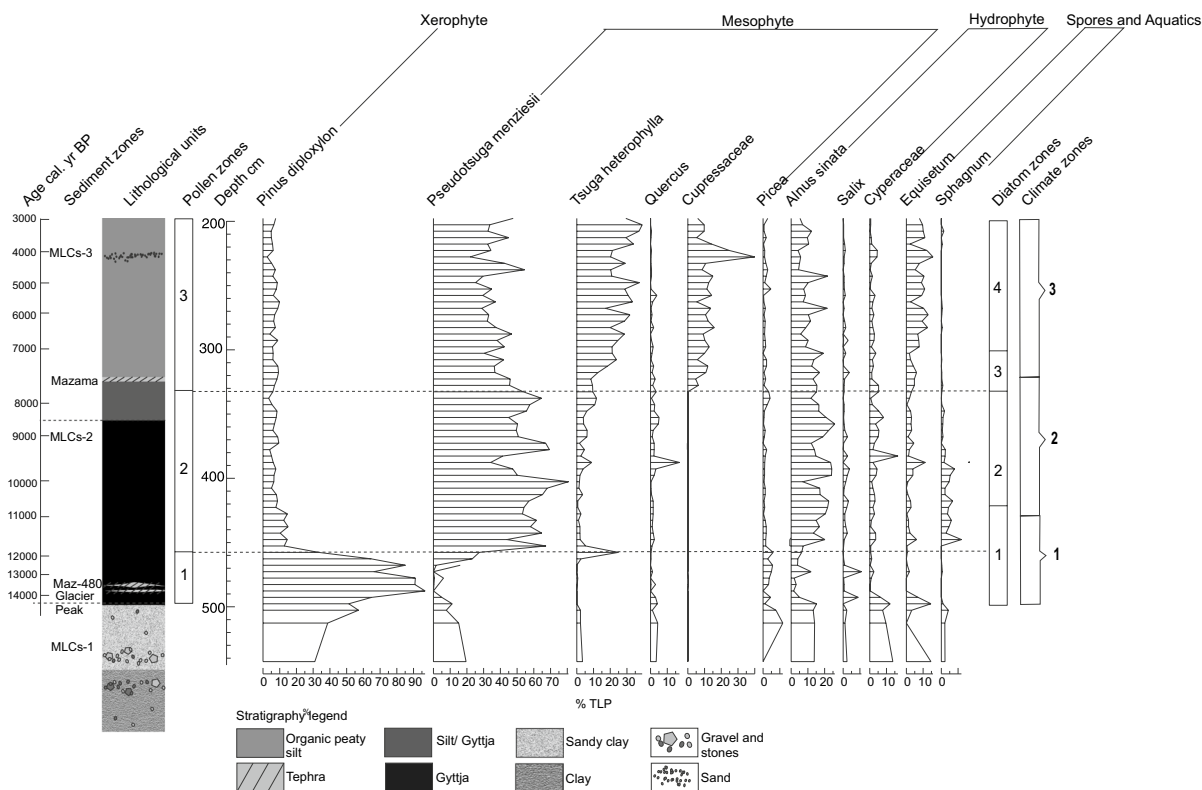


Fig. 7 Summary pollen assemblage from Moss Lake (% total land pollen) (adapted from Egan et al. 2016) showing the major shifts in vegetation through the Holocene in relation to

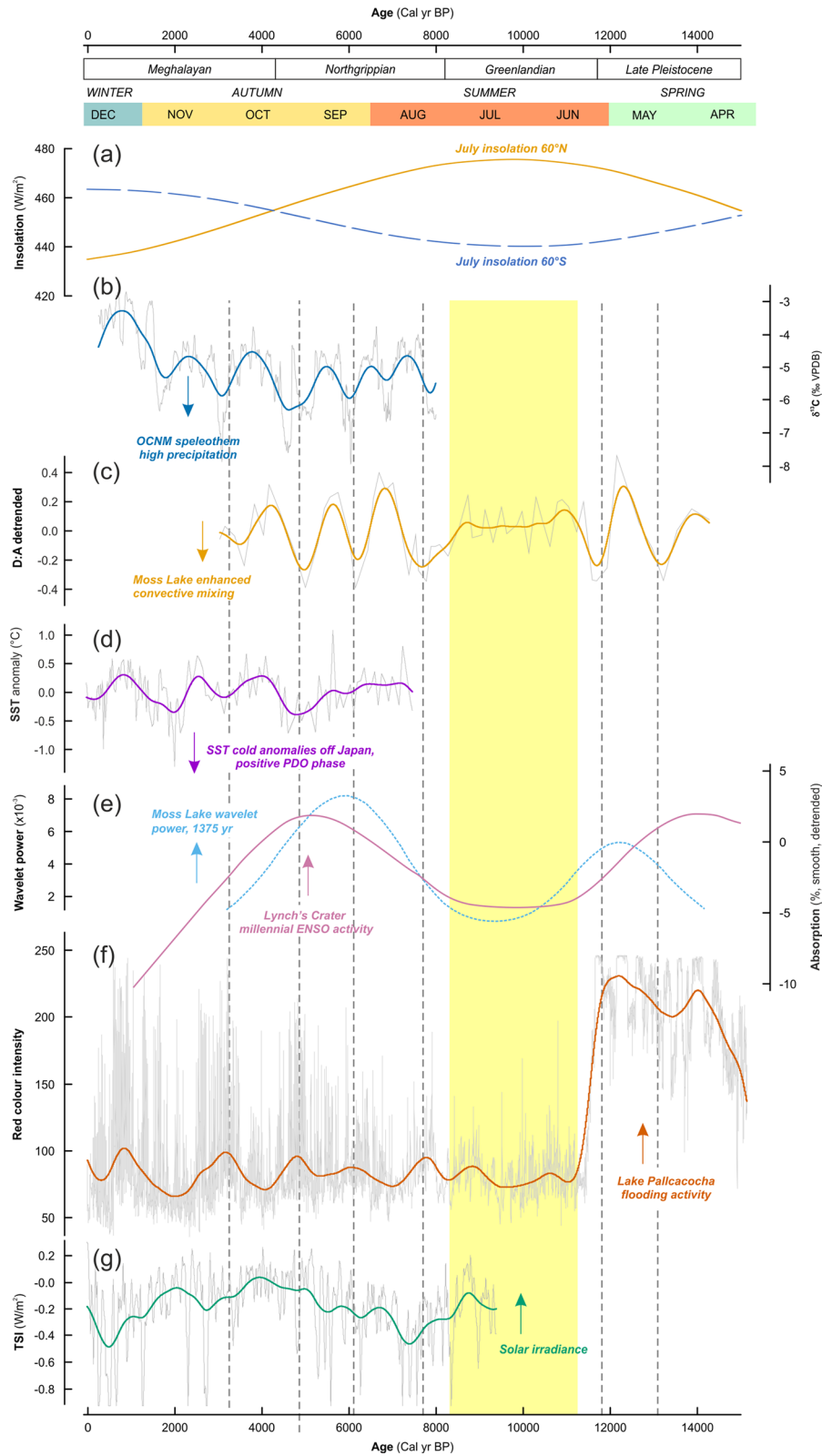
the lithological, diatom and climate zones identified in this paper. Pollen zones have been identified and are referred to in the text as MLCp-1, MLCp-2 and MLCp-3

Millennial variability in the Pacific Northwest

A highly significant ~1400-year oscillation is prominent in the Late Glacial (14,200–11,500 cal year BP) and much of the Northgrippian and Meghalayan (8500–3000 cal year BP). Associated shifts in climate conditions, which affected convective mixing, are inferred, with alternating episodes of water column stability and convective mixing. It is important to stress here that because of the lack of quantitative framing for the specific teleconnections, it is impossible to determine exact forcings, and mechanisms such as ENSO and PDO are suggested as possibilities. Millennial-scale peaks in wind-driven convection and mixing are shown in Fig. 8 (vertical dashed lines). The periodicity and duration of the mixing phases correlate well with climate changes recorded in speleothems from southwestern Oregon (Fig. 8b). Ersek et al. (2012) reported statistically significant fluctuations in the OCN02-1 speleothem

$\delta^{13}\text{C}$ values (precipitation and biomass proxy) at 1500-year and 500-year periodicities, as well as a 2000-year periodicity in $\delta^{18}\text{O}$ (temperature proxy). The high-resolution $\delta^{13}\text{C}$ record displays a series of high-amplitude negative excursions interpreted as extreme cold-wet events, which correspond well, within age-model and resolution uncertainties, with millennial-scale peaks in wind-driven convection at Moss Lake (Fig. 8b). The comparison of the low-frequency component of the records supports a coherent linkage between enhanced wintertime precipitation and increased windiness in the PNW, likely associated with the shifting position and intensity of the wintertime storm tracks. This millennial oscillation, to our knowledge, has not been documented previously in biotic lake proxies in the region, although a 1400-year cycle was reported from lake records and peatland initiation dates in adjacent interior western Canada (Campbell et al. 2000).

Fig. 8 Millennial climate fluctuations at Moss Lake in the Pacific context, showing: **a** perihelion season and orbital forcing parameters (Berger 1978); **b** speleothem stable carbon isotope data from Oregon Caves National Monument (Ersek et al. 2012); **c** Moss Lake diatom-based convective mixing proxy (detrended D:A ratio, this study); **d** North Pacific sea surface temperature anomalies off Japan (residuals from 3rd order polynomial fitting) (Isono et al. 2009); **e** comparison of the Moss Lake wavelet power at period 1375 year (blue dotted line, this study) and long-term peat absorption at Lynch’s Crater, Northern Australia (pink line, Turney et al. 2004); **f** sediment record of flooding activity at Lake Pallcacocha, Ecuador (Moy et al. 2002); **g** TSI data (total solar irradiance) (Steinhilber et al. 2012). Bold lines in **b, c, d, f, g** show a consistent lowpass filtering to highlight millennial-scale dynamics in the records. Yellow shaded interval corresponds to the boreal summer insolation maximum and weakening of millennial activity at Moss Lake. Dashed vertical lines correspond to minima in the Moss Lake D:A ratio and coherent cold-wet-windy millennial episodes in the PNW. (Color figure online)



In terms of climatological mechanisms underpinning the millennial fluctuations, a prevailing Western position and weakly developed Aleutian Low (Fig. 1) may have contributed to wet and windy phases. Both Moss Lake and the Oregon Caves National Monument sites are located within a geographical sector where wintertime precipitation is negatively correlated with the PDO (Ersek et al. 2012), supporting a common response to past variability linked to wider atmospheric dynamics over the North Pacific and a potential linkage to ENSO dynamics in the tropical Pacific. Ersek et al. (2012) highlighted the similarity between centennial and millennial periodic components in the Oregon speleothems and those in a climate simulation of the Pacific Ocean–atmosphere system (Emile-Geay et al. 2007). Based on present-day teleconnections, colder, wetter, windier episodes in the PNW may have been associated with weaker or less frequent El Niño events. Considering these teleconnections on a much larger spatial scale, we also note a good match between the 1500-year Holocene fluctuations reported in mid-latitude North Pacific sea surface temperatures (Isono et al. 2009) and the PNW records (Fig. 8b–d). This match further supports a wider pattern of millennial dynamics linked to PDO-like variability in the coupled Pacific Ocean–atmosphere system. Cooling in the high-resolution MD01-2421 record off Japan, in opposition to warming on the Californian Pacific margin, reflects variation in the North Pacific sub-tropical gyre system (Isono et al. 2009; Barron et al. 2003). SST cooling anomalies at this location are linked to weakening of the Kuroshio Extension jet associated with a weaker sub-arctic gyre or stronger subtropical gyre (Isono et al. 2009), which in turn may be associated with PDO-like dynamics, as well as the North Pacific Gyre Oscillation (NPGO). Overall, these records point to a coherent pattern of millennial fluctuations during much of the Holocene.

Upon visual inspection, a potential linkage to millennial ENSO-like dynamics is also supported by the significant non-stationarity in the Moss Lake oscillation during the Greenlandian. The absence of significant millennial fluctuations at Moss Lake around the peak in boreal summer insolation (Fig. 8, yellow shading) is consistent with modelling of ENSO under different insolation conditions (Clement et al. 2001), whereby the maximum hemispheric asymmetry in insolation, experienced when perihelion is

in summer to early autumn (Fig. 8a), enhances the cross-equatorial zonal temperature gradient, increasing the trade winds and suppressing El Niño events. These dynamics may underpin a semi-precessional timescale of strengthening and weakening ENSO-like dynamics according to changes in the hemispheric insolation gradient, occurring twice within each precession (19/21 k year) cycle (Tudhope et al. 2001; Turney et al. 2004). The power of the millennial oscillation at Moss Lake (Fig. 8d) matches closely the long-term variability in the peat humification record at Lynch’s Crater in Northern Australia (Fig. 8e), a proxy for hydrological changes linked to past millennial ENSO activity (Turney et al. 2004). Notably, we observe a common strengthening of the signals at times of reduced insolation gradient, during spring and autumn perihelion. The diminishment of ENSO activity during the Greenlandian was reported previously at Laguna Pallcacocha in Ecuador (Moy et al. 2002). A common pattern of weak millennial variability between Moss Lake and Laguna Pallcacocha is observed (Fig. 8f), with diminished amplitude of changes during the Greenlandian, preceded and followed by phases of enhanced millennial variability in both records. We note that recent research raises questions around the interpretation of the Pallcacocha record in terms of the connection and phasing between high-precipitation events, flooding frequency, and El Niño/La Niña states at the site, and indeed within complex climatological patterns over Ecuador (Schneider et al. 2018). Nevertheless, the correspondence between millennial fluctuations in PNW climate and flooding episodes at Pallcacocha is striking and points to significant temperate-tropical interactions on millennial timescales, even if the dynamics may not be directly comparable to interannual ENSO patterns. We recognise also that a wider debate has emerged around whether ENSO dynamics were weakest during the Greenlandian or Northgrippian (Carré et al. 2021). Nevertheless, without attempting to infer a single unifying pattern of ENSO dynamics for all areas and timescales, we note several other records that demonstrate either a Greenlandian weakening/absence of ENSO activity and/or a late Northgrippian and Meghalayan increase in ENSO-like intensity (Kennett et al. 2007; Barron and Anderson, 2011; Jiménez-Moreno et al. 2019). Our findings of strong millennial variability during the Late Pleistocene at Moss Lake are also consistent

with ENSO-teleconnected dynamics detected in the Late Pleistocene in eastern North America (Rittenour et al. 2000), prior to the summer insolation maximum. Alternatively, the diminished millennial signal observed in the Greenlandian at Moss Lake may be partly controlled and/or exacerbated by local factors, in particular, terrestriation of the lake during the Greenlandian and early Northgrippian.

The underlying forcing and pacing of Holocene millennial variability remain debated, and a full evaluation is beyond the scope of this discussion. However, we note a close match in frequency/periodicity with North Atlantic ice-rafting episodes, typically discussed as a 1470-year cycle, but more specifically as 1374 ± 502 year for the Holocene (Bond et al. 1999). Thus, it is possible that the PNW dynamics could be influenced by high-latitude and North Atlantic dynamics. Climate modelling by Liu et al. (2014), for example, supports teleconnections between deglaciation and meltwater pulses, atmospheric CO₂ changes, and ENSO amplitude. However, we do not find a consistent phasing with specific Holocene episodes of ice-rafting (Bond events) and note that other studies highlight the non-stationarity of this oscillation in the Bond datasets and suggest a mixed origin (averaging of ~1000- and ~2000-year cycles) for the ~1400 year cycle. We also note a fundamental difference between the high amplitude and magnitude of Greenlandian (early Holocene) climate anomalies in the North Atlantic realm (e.g., 8.2-ka and 9.3-ka events) and weakening of millennial dynamics at Moss Lake and in other Pacific records (Fig. 8). This difference points instead to a likely Pacific origin for climate fluctuations in the PNW.

Several studies suggest that centennial and millennial fluctuations in the Pacific Ocean–atmosphere system may be driven by changes in solar irradiance forcing (Emile-Geay et al. 2007; Marchitto et al. 2010), and indeed that ENSO dynamics may represent a major factor for amplification of weak solar forcing changes within the Earth system. In their study of the high-resolution Oregon speleothem records, Ersek et al. (2012) proposed an association of cold-wet events with intervals of high solar activity, mediated by ENSO-like responses to changes in solar forcing in the tropical Pacific. When the Moss Lake D:A ratio is compared to the Holocene total solar irradiance (TSI) Record (Steinhilber et al. 2012), it is evident that there are some similarities in

the records. For example, *D. pseudostelligera* abundances spike close to 7500 cal year BP, 6000 cal year BP and 4500 cal year BP, corresponding with solar irradiance declines (grand solar minima) (Fig. 8g, Steinhilber et al. 2012), consistent with the pattern reported by Ersek et al. (2012). However, consistent phasing across the records at millennial timescales is not observed, and indeed a 1400-year or 1500-year cycle is generally not detected in direct solar proxies (Debret et al. 2007). This points to a complex influence of solar forcing on the climate system, involving slow changes in the ocean system, integration of forcing over long time periods and non-linear response dynamics. During the Greenlandian, the forcing for the weak, ~450-year oscillation may also reside in solar variability. Steinhilber et al. (2012) revealed significant periodicities of 350 and 500 years in the TSI reconstruction, which also vary in amplitude throughout time and are prominent during times of solar minima.

Conclusions

The diatom record from Moss Lake agrees with the previously published pollen record that revealed long-term (sub-orbital-scale) climate and vegetation shifts during the onset of the Holocene, with a cold and dry climate in the Late Pleistocene (GI-1, GS-1), shift to warmer conditions in the Greenlandian, maximum warmth in the Northgrippian, and cooler and moist conditions in the Meghalayan. Importantly, the diatom assemblages reveal sensitive limnological responses to Holocene climate-driven environmental changes in the PNW that were not evident in the pollen record and have not been previously documented in aquatic-based paleoecological studies. We propose that the *D. pseudostelligera*:*Aulacoseira* ratio is a meaningful ecological indicator for wind-driven, convective mixing at Moss Lake. Time series analyses on the D:A ratio identified a dominant millennial periodicity near 1400 years, which is interpreted to reflect, in large part, wind intensity changes conceptually linked to coherent PNW climate variability and wider Pacific Ocean–atmosphere teleconnections. The wavelet analysis highlights a marked change in the dominant timescale of climate variability in the Late Pleistocene (high-amplitude events, 1400-year periodicity), Greenlandian/early Northgrippian

(low-amplitude events, ~450-year periodicity) and the late Northgrippian/Meghalayan (high-amplitude events, 1400-year periodicity). The record from Moss Lake reveals near-identical periodicities to those reported from the speleothem record in southwestern Oregon (Ersek et al. 2012) and consistent patterns of millennial-scale variability over the Holocene. These similarities in frequency and amplitude point to a common influence of storm-track variations over the PNW, associated with past ENSO-like dynamics. The weakening of millennial variability at Moss Lake during the Greenlandian is consistent with semi-precessional forcing of ENSO-like dynamics in the wider Pacific region. However, several other records indicate suppression of ocean–atmosphere teleconnections during the Northgrippian, suggesting that other drivers may be influential in the PNW, or that the sensitivity of the lake record to different climate oscillations may change over time because of catchment-scale endogenic processes. Furthermore, there is a possibility that the ~450-year periodicity is an artefact of sample noise, so caution is taken with this interpretation. This study successfully demonstrated millennial and multi-centennial-scale ocean–atmosphere teleconnection variability in Washington, contributing to our understanding of ocean–atmosphere interactions throughout the Holocene. Further studies with high analytical resolution in the wider PNW can enhance knowledge of past ocean–atmosphere teleconnection variability and further elucidate the sensitivity of different natural systems and climate proxy variables. Whilst this approach has proven useful in a shallow lake, deeper lakes with strong temperature gradients merit further investigation.

Acknowledgements This work was supported by the NERC Radiocarbon Facility NRCF010001 (Allocation Numbers 1877.1014; 1728.1013). We thank Danielle Alderson (The University of Manchester), Douglas Clark (Western Washington University) and Harold N. Wershow (Western Washington University) for assistance in the field.

Author contributions JE curated the research topic, designed the research, performed the analyses, and wrote the original draft of the paper. WJF advised on spectral analyses, reviewed and edited the manuscript. TEHA advised on diatom analysis, reviewed and edited the manuscript.

Data availability Data series reconstructed in this study is deposited at “PANGAEA. Data Publisher for Earth & Environmental Science” (<https://doi.pangaea.de/10.1594/PANGAEA.918535>), or users can also contact the authors for more

information on data series. Egan et al. (2020) Postglacial diatom-climate responses in a small lake in the Pacific Northwest of North America—Cores collected from Moss Lake, WA, USA have been analysed for diatoms and pollen as well as LOI and magnetic susceptibility, age/depth model output, PAN-GAEA. Data Publisher for Earth & Environmental Science, <https://doi.pangaea.de/10.1594/PANGAEA.918535>

Declarations

Conflict of interest The authors declare that they have no conflict of interest.

Open Access This article is licensed under a Creative Commons Attribution 4.0 International License, which permits use, sharing, adaptation, distribution and reproduction in any medium or format, as long as you give appropriate credit to the original author(s) and the source, provide a link to the Creative Commons licence, and indicate if changes were made. The images or other third party material in this article are included in the article’s Creative Commons licence, unless indicated otherwise in a credit line to the material. If material is not included in the article’s Creative Commons licence and your intended use is not permitted by statutory regulation or exceeds the permitted use, you will need to obtain permission directly from the copyright holder. To view a copy of this licence, visit <http://creativecommons.org/licenses/by/4.0/>.

References

- Anderson L, Abbott MB, Finney BP, Burns SJ (2005) Regional atmospheric circulation change in the North Pacific during the Holocene inferred from lacustrine carbonate oxygen isotopes, Yukon Territory, Canada. *Quat Res* 64:21–35
- Barron JA, Anderson L (2011) Enhanced Late Holocene ENSO/PDO expression along the margins of the eastern North Pacific. *Quat Int* 235:3–12
- Barron JA, Heusser L, Herbert T, Lyle M (2003) High-resolution climatic evolution of coastal northern California during the past 16,000 years. *Paleoceanography* 18:1–24
- Bennett KD (2007) Psimpoll and Pscomb programs for plotting and analysis. <http://www.chrono.qub.ac.uk/psimpoll/psimpoll.html>, Accessed 3 May 2020
- Bennett JR, Cumming BF, Leavitt PR, Chiu M, Smol JP, Szeicz J (2001) Diatom, pollen, and chemical evidence of postglacial climatic change at big lake, South-Central British Columbia, Canada. *Quat Res* 55:332–343
- Bennion H, Carvalho L, Sayer CD, Simpson GL, Wischniewski J (2012) Identifying from recent sediment records the effects of nutrients and climate on diatom dynamics in Loch Leven. *Freshw Biol* 57:2015–2029
- Berger A (1978) Long-term variations of daily insolation and quaternary climatic changes. *J Atmos Sci* 35:2362–2367
- Bond GC, Showers W, Elliot M, Evans M, Lotti R, Hajdas I, Bonani G, Johnson S (1999) The North Atlantic’s 1–2 kyr climate rhythm: relation to Heinrich events, Dansgaard/Oeschger cycles and the Little Ice Age. *Geophys Monogr-Am Geophys Union* 112:35–58

- Bradbury JP, Colman SM, Dean WE (2004) Limnological and climatic environments at Upper Klamath Lake, Oregon during the past 45 000 years. *J Paleolimnol* 31:167–188
- Bronk Ramsey C (2021) OxCal V. 4.4. <https://c14.arch.ox.ac.uk/oxcal/OxCal.html>. Accessed 14 July 2021
- Bunn A, Korpela M, Biondi F, Campelo F, Mérian P, Qeadan F, Zang C (2021) dplR: dendrochronology program library in R. R package version 1.7.2. <https://CRAN.R-project.org/package=dplR>. Accessed 20 Sept 2021
- Campbell ID, Campbell C, Yu Z, Vitt DH, Apps MJ (2000) Millennial-scale rhythms in peatlands in the western interior of Canada and in the global carbon cycle. *Quat Res* 54:155–158
- Carré M, Braconnot P, Elliot M, D’agostino R, Schurer A, Shi X, Marti O, Lohmann G, Jungclaus J, Cheddadi R, Di Carlo IA (2021) High-resolution marine data and transient simulations support orbital forcing of ENSO amplitude since the mid-Holocene. *Quat Sci Rev* 268:107125
- Clement AC, Cane MA, Seager R (2001) An orbitally driven tropical source for abrupt climate change. *J Clim* 14:2369–2375
- Courtney Mustaphi CJ, Pisaric MFJ (2014) Holocene climate–fire–vegetation interactions at a subalpine watershed in southeastern British Columbia, Canada. *Quat Res* 81:228–239
- Dean WE (1974) Determination of carbonate and organic matter in calcareous sediments and sedimentary rocks by loss on ignition; comparison with other methods. *J Sediment Res* 44:242–248
- Debret M, Bout-Roumzeilles V, Grousset F, Desmet M, McManus JF, Massei N, Sebag D, Petit JR, Copard Y, Trentesaux A (2007) The origin of the 1500-year climate cycles in Holocene North-Atlantic records. *Clim past* 3:569–575
- Descamps-Julien B, Gonzalez A (2005) Stable coexistence in a fluctuating environment: an experimental demonstration. *Ecology* 86:2815–2824
- Egan J, Staff R, Blackford J (2015) A high-precision age estimate of the Holocene Plinian eruption of Mount Mazama, Oregon, USA. *Holocene* 25:1054–1067
- Egan J, Fletcher WJ, Allott TEH, Lane CS, Blackford JJ, Clark DH (2016) The impact and significance of tephra deposition on a Holocene forest environment in the North Cascades, Washington, USA. *Quat Sci Rev* 137:135–155
- Egan J, Allott TEH, Blackford JJ (2019) Diatom-inferred aquatic impacts of the mid-Holocene eruption of Mount Mazama, Oregon, USA. *Quat Res* 91:163–178
- Egan J, Fletcher WJ, Allott TEH (2020) PANGAEA: postglacial diatom-climate responses in a small lake in the Pacific Northwest of North America - Cores collected from Moss Lake, WA, USA have been analysed for diatoms and pollen as well as LOI and magnetic susceptibility, age/depth model output. <https://doi.org/10.1594/PANGAEA.918535>. Accessed 25 May 2022
- Emile-Geay J, Cane M, Seager R, Kaplan A, Almasi P (2007) El Niño as a mediator of the solar influence on climate. *Paleoceanography* 22:1–16
- Ersek V, Clark PU, Mix AC, Cheng H, Edwards RL (2012) Holocene winter climate variability in mid-latitude western North America. *Nat Commun* 3:1219
- Galloway JM, Wigston A, Patterson RT, Swindles GT, Reinhardt E, Roe HM (2013) Climate change and decadal to centennial-scale periodicities recorded in a late Holocene NE Pacific marine record: examining the role of solar forcing. *Palaeogeogr Palaeoclimatol Palaeoecol* 386:669–689
- Gavin DG, Henderson ACG, Westover KS, Fritz SC, Walker IR, Leng MJ, Hu FS (2011) Abrupt Holocene climate change and potential response to solar forcing in western Canada. *Quat Sci Rev* 30:1243–1255
- Hammer Ø, Harper DA, Ryan PD (2001) PAST: paleontological statistics software package for education and data analysis. *Palaeontol Electron* 4:1–9
- Iizumi T, Luo JJ, Challinor AJ, Sakurai G, Yokozawa M, Sakuma H, Brown ME, Yamagata T (2014) Impacts of El Niño Southern Oscillation on the global yields of major crops. *Nat Commun* 5:1–7
- Isono D, Yamamoto M, Irino T, Oba T, Murayama M, Nakamura T, Kawahata H (2009) The 1500-year climate oscillation in the midlatitude North Pacific during the Holocene. *Geology* 37:591–594
- Jiménez-Moreno G, Anderson RS, Shuman BN, Yackulic E (2019) Forest and lake dynamics in response to temperature, North American monsoon and ENSO variability during the Holocene in Colorado (USA). *Quat Sci Rev* 211:59–72
- Karst-Riddoch TL, Pisaric MFJ, Youngblut DK, Smol JP (2005) Postglacial record of diatom assemblage changes related to climate in an alpine lake in the northern Rocky Mountains, Canada. *Can J Bot* 83:968–982
- Kennett DJ, Kennett JP, Erlandson JM, Cannariato KG (2007) Human responses to Middle Holocene climate change on California’s Channel Islands. *Quat Sci Rev* 26:351–367
- Krammer K, Lange-Bertalot H (1991) Süßwasserflora von Mitteleuropa vol 2/4 Bacillariophyceae. Gustav Fischer Verlag, Stuttgart
- Krammer K, Lange-Bertalot H (1999a) Süßwasserflora von Mitteleuropa vol 2/1 Bacillariophyceae. Spektrum Akademischer verlag GmbH, Berlin
- Krammer K, Lange-Bertalot H (1999b) Süßwasserflora von Mitteleuropa vol 2/2 Bacillariophyceae. Spektrum Akademischer verlag GmbH, Berlin
- Liu Z, Lu Z, Wen X, Otto-Bliessner BL, Timmermann A, Cobb KM (2014) Evolution and forcing mechanisms of El Niño over the past 21,000 years. *Nature* 515:550–553
- Lotter AF, Bigler C (2000) Do diatoms in the Swiss Alps reflect the length of ice-cover? *Aquat Sci* 62:125–141
- Mantua NJ, Hare SR, Zhang Y, Wallace JM, Francis RC (1997) A Pacific interdecadal climate oscillation with impacts on salmon production. *Bull Am Meteorol Soc* 78:1069–1080
- Marchitto TM, Muscheler R, Ortiz JD, Carriquiry JD, van Geen A (2010) Dynamical response of the tropical Pacific Ocean to solar forcing during the early Holocene. *Science* 330:1378–1381
- Moy CM, Seltzer GO, Rodbell DT, Anderson DM (2002) Variability of El Niño/Southern Oscillation activity at millennial timescales during the Holocene epoch. *Nature* 420:162–165
- Prichard SJ, Gedalof Z, Oswald WW, Peterson DL (2009) Holocene fire and vegetation dynamics in a montane

- forest, North Cascade Range, Washington, USA. *Quat Res* 72:57–67
- Reimer PJ, Austin WE, Bard E, Bayliss A, Blackwell PG, Ramsey CB, Butzin M, Cheng H, Edwards RL, Friedrich M, Grootes PM (2020) The IntCal20 Northern Hemisphere radiocarbon age calibration curve (0–55 cal kBP). *Radiocarbon* 62:725–757
- Rigg GB (1958) Peat resources of Washington, USGS Bulletin No. 44, Olympia, WA. https://www.dnr.wa.gov/Publications/ger_b44_peat_reasources_wa_1.pdf. Accessed 4 May 2020
- Rittenour TM, Brigham-Grette J, Mann ME (2000) El Niño-like climate teleconnections in New England during the late Pleistocene. *Science* 288:1039–1042
- Roesch A, Schmidbauer H (2018) WaveletComp: computational wavelet analysis. R package version 1.1. <https://CRAN.R-project.org/package=WaveletComp>. Accessed 20 Sept 2021
- Rodionov SN, Bond NA, Overland JE (2007) The Aleutian Low, storm tracks, and winter climate variability in the Bering Sea. *Deep Sea Res 2 Top Stud Oceanogr* 54:2560–2577
- Rodionov SN, Overland JE, Bond NA (2005) Spatial and temporal variability of the Aleutian climate. *Fish Oceanogr* 14:3–21
- Rühland K, Priesnitz A, Smol JP (2003) Paleolimnological evidence from diatoms for recent environmental changes in 50 lakes across Canadian Arctic Treeline. *Arct Antarct Alp Res* 35:110–123
- Saros JE, Stone JR, Pederson GT, Slemmons KE, Spanbauer T, Schliep A, Cahl D, Williamson CE, Engstrom DR (2012) Climate-induced changes in lake ecosystem structure inferred from coupled neo-and paleoecological approaches. *Ecology* 93:2155–2164
- Schmidt R, Kamenik C, Lange-Bertalot H, Klee R (2004) *Fragilaria* and *Staurosira* (Bacillariophyceae) from sediment surfaces of 40 lakes in the Austrian Alps in relation to environmental variables, and their potential for palaeoclimatology. *J Limnol* 63:171–189
- Schneider T, Hampel H, Mosquera PV, Tylmann W, Grosjean M (2018) Paleo-ENSO revisited: Ecuadorian Lake Pallacocha does not reveal a conclusive El Niño signal. *Glob Planet Change* 168:54–66
- Schulz M, Mudelsee M (2002) REDFIT: estimating red-noise spectra directly from unevenly spaced paleoclimatic time series. *Comput Geosci* 28:421–426
- Signal developers (2013) Signal: signal processing. R package version 0.7–7. <http://r-forge.r-project.org/projects/signal/>. Accessed 20 Sept 2021
- Spaulding SA, Bishop IW, Edlund MB, Lee S, Furey P, Jovanovska E, Potapova M (2021) Diatoms.org. <https://diatoms.org/>. Accessed 14 July 2021
- Staff RA, Bronk Ramsey C, Bryant CL, Brock F, Payne RL, Schlolaut G, Marshall MH, Brauer A, Lamb HF, Tarasov P, Yokoyama Y, Haraguchi T, Gotanda K, Yonenobu H, Nakagawa T, Members (2011) New 14C determinations from Lake Suigetsu, Japan: 12,000 to 0 cal BP. *Radiocarbon* 53:511–528
- Steinhilber F, Abreu JA, Beer J, Brunner I, Christl M, Fischer H, Heikkilä U, Kubik PW, Mann M, McCracken KG, Miller H, Miyahara H, Oerter H, Wilhelms F (2012) 9,400 years of cosmic radiation and solar activity from ice cores and tree rings. *Proc Natl Acad Sci USA* 109:5967–5971
- Steinman BA, Abbott MB, Mann ME, Ortiz JD, Feng S, Pompeani DP, Stansell ND, Anderson L, Finney BP, Bird BW (2014) Ocean-atmosphere forcing of centennial hydroclimate variability in the Pacific Northwest. *Geophys Res Lett* 41:2553–2560
- Steinman BA, Pompeani DP, Abbott MB, Ortiz JD, Stansell ND, Finkenbinder MS, Mihindukulasooriya LN, Hillman AL (2016) Oxygen isotope records of Holocene climate variability in the Pacific Northwest. *Quat Sci Rev* 142:40–60
- Stone JR, Saros JE, Pederson GT (2016) Coherent late-Holocene climate-driven shifts in the structure of three Rocky Mountain lakes. *Holocene* 26:1103–1111
- Stone JR, Saros JE, Spanbauer TL (2019) The influence of fetch on the Holocene thermal structure of Hidden Lake, Glacier National Park. *Front Earth Sci* 7:28
- Thomson DJ (1990) Time series analysis of Holocene climate data. *Philos Trans A* 330:601–616
- Torrence C, Compo GP (1998) A practical guide to wavelet analysis. *Bull Am Meteorol Soc* 79:61–78
- Tudhope AW, Chilcott CP, McCulloch MT, Cook ER, Chappell J, Ellam RM, Lea DW, Lough JM, Shimmield GB (2001) Variability in the El Niño-Southern Oscillation through a glacial-interglacial cycle. *Science* 291:1511–1517
- Turney CS, Kershaw AP, Clemens SC, Branch N, Moss PT, Fifield LK (2004) Millennial and orbital variations of El Niño/Southern Oscillation and high-latitude climate in the last glacial period. *Nature* 428:306–310
- Wang L, Li J, Lu H, Gu Z, Rioual P, Hao Q, Mackay AW, Jiang W, Cai B, Xu B, Han J, Chu G (2012) The East Asian winter monsoon over the last 15,000 years: its links to high-latitudes and tropical climate systems and complex correlation to the summer monsoon. *Quat Sci Rev* 32:131–142
- Weedon G (2003) Time-series analysis and cyclostratigraphy: examining stratigraphic records of environmental cycles. Cambridge University Press, Cambridge
- Whitlock C (1992) Vegetational and climatic history of the Pacific Northwest during the last 20,000 years: Implications for understanding present-day biodiversity. *Northwest Environ J* 8:5–28

Publisher's Note Springer Nature remains neutral with regard to jurisdictional claims in published maps and institutional affiliations.